Electronic Supplementary Material (ESI) for Dalton Transactions.


# $RuO_2$ nanoparticles anchored on g-$C_3N_4$ as an efficient bifunctional electrocatalyst for water splitting in acidic media

Yun Wu, Rui Yao, Qiang Zhao, Jinping Li, Guang Liu*

Shanxi Key Laboratory of Gas Energy Efficient and Clean Utilization, College of Chemical Engineering and Technology, Taiyuan University of Technology, Taiyuan, Shanxi 030024, PR China.

**Supplementary figures and tables**

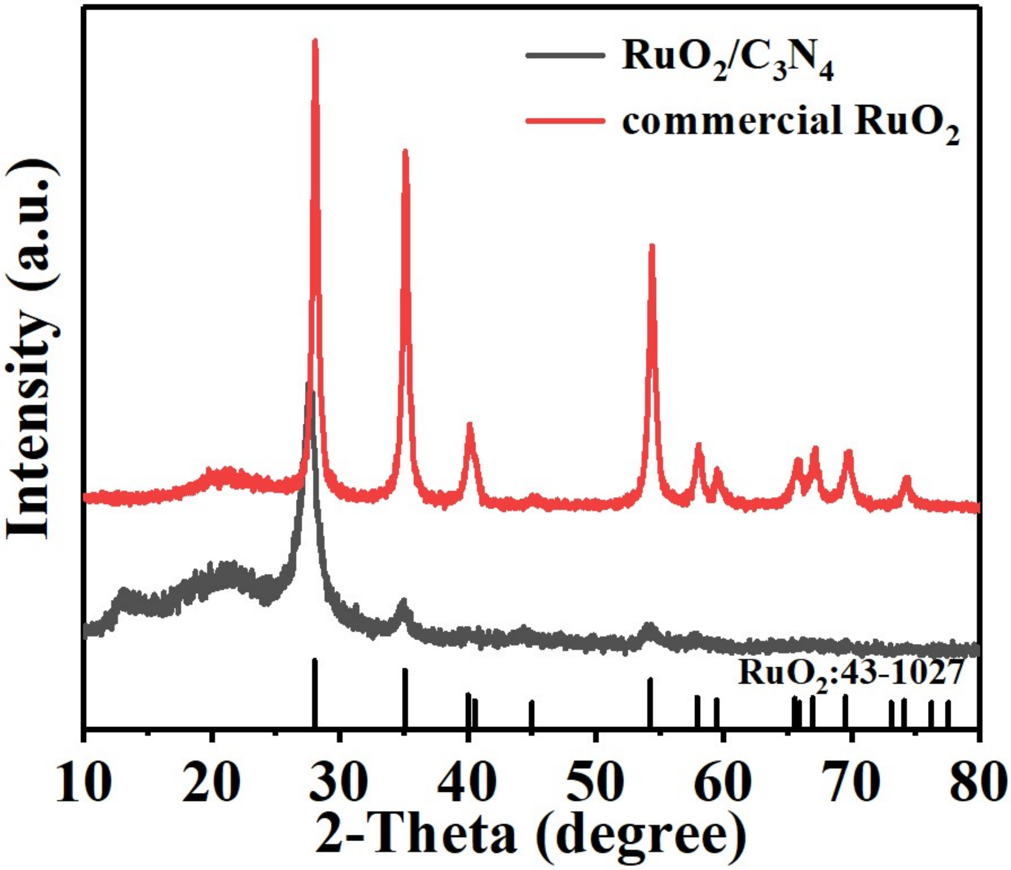


Figure S1. XRD image of $RuO_2/C_3N_4$ and commercial $RuO_2$.

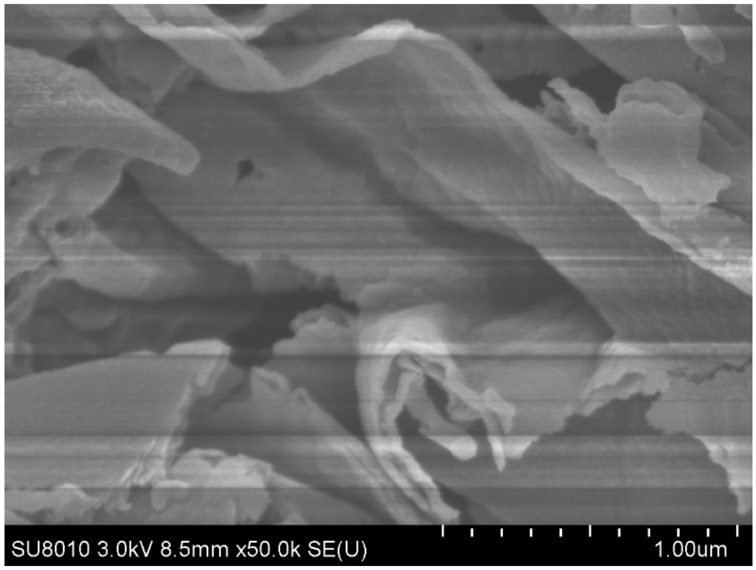


Figure S2. SEM image of g-$C_3N_4$.

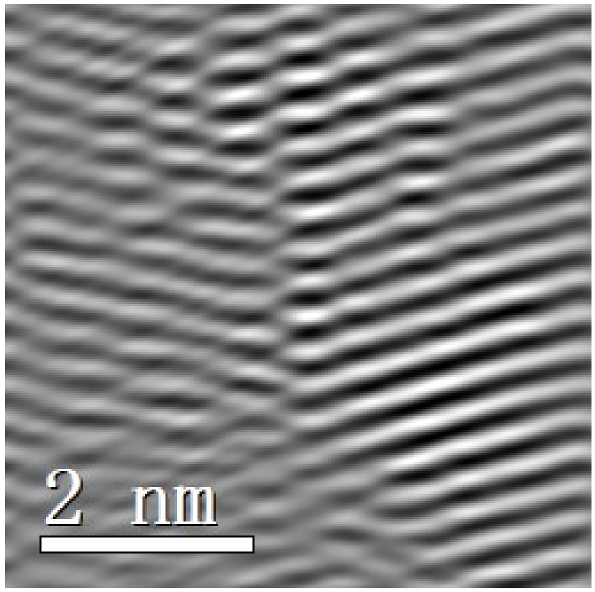

Figure S3. Inverse fast Fourier transform (IFFT) image of $RuO_2/C_3N_4$.

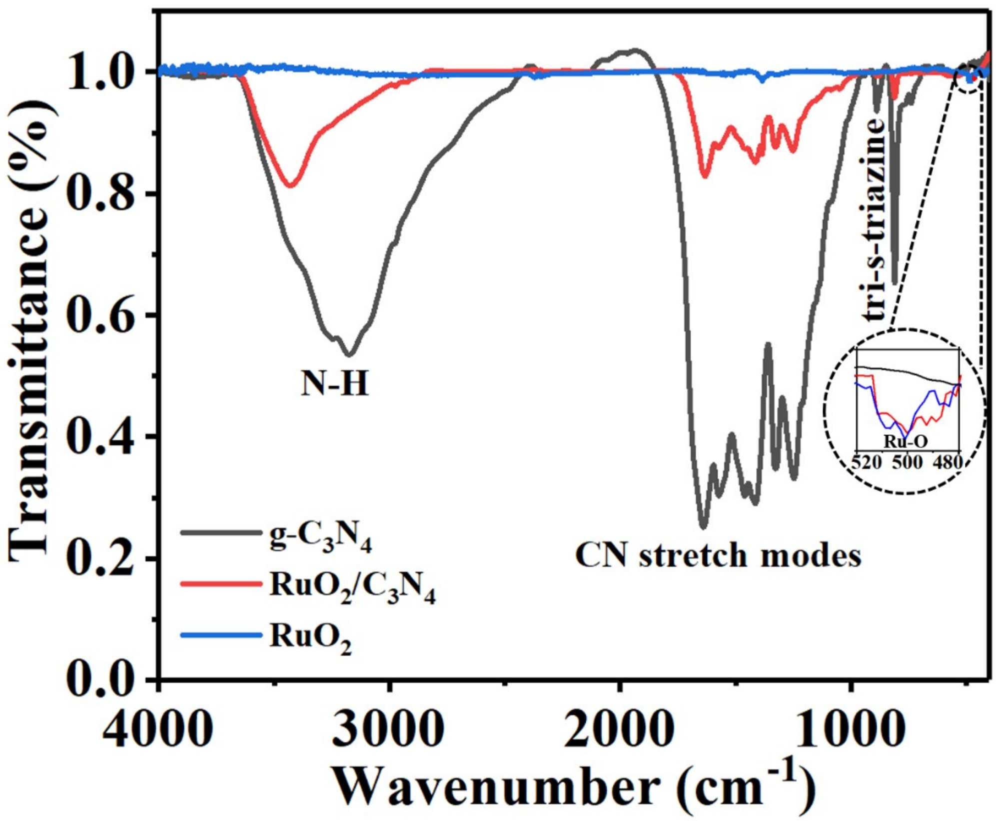


Figure S4. Fourier transform infrared spectroscopy (FT-IR) image of $RuO_2/C_3N_4$, $RuO_2$ and g-$C_3N_4$.

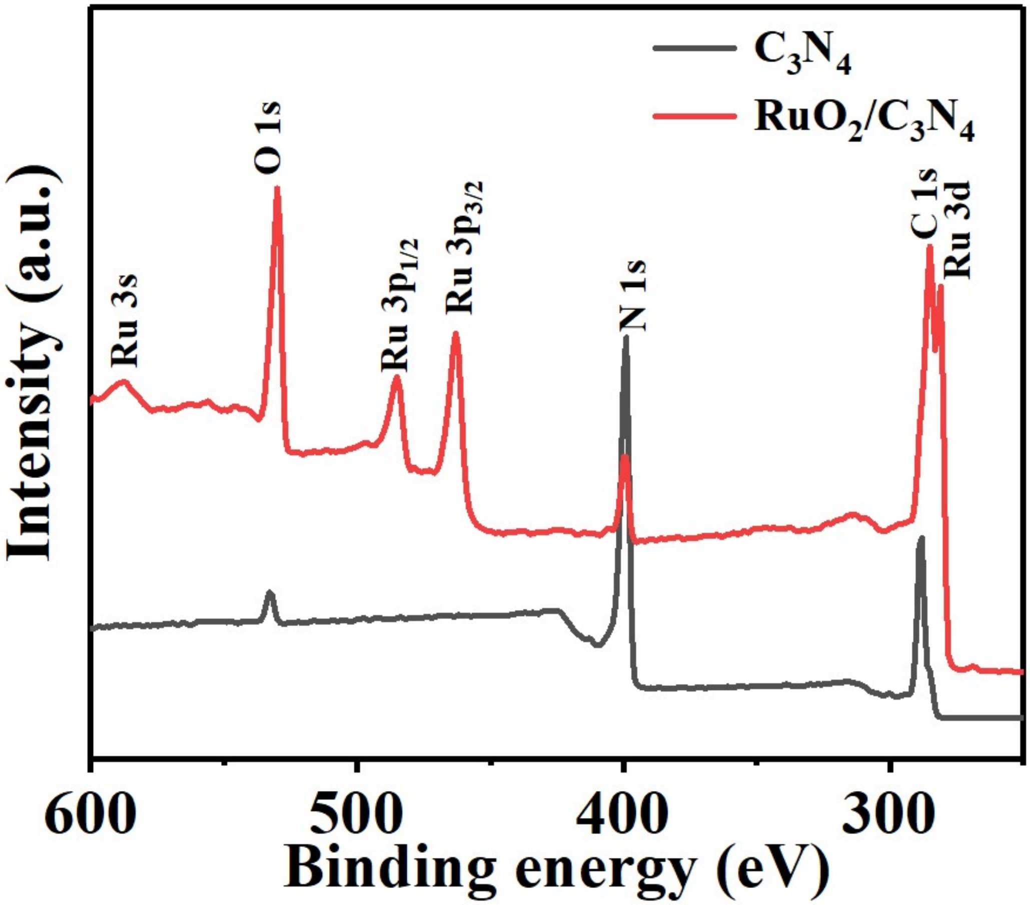

Figure S5. XPS survey pattern of $RuO_2/C_3N_4$ and g-$C_3N_4$.

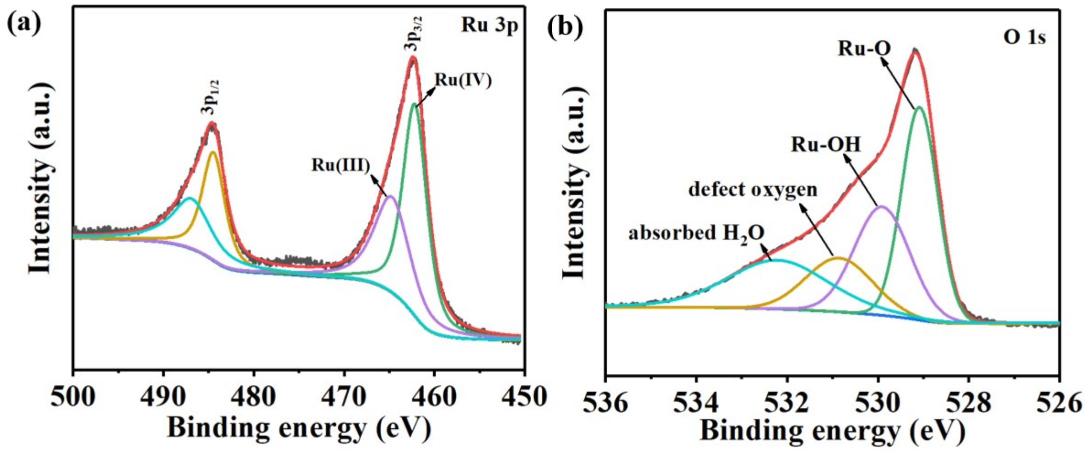


Figure S6. a) Ru 3p, b) O 1s XPS spectra of bare $RuO_2$.

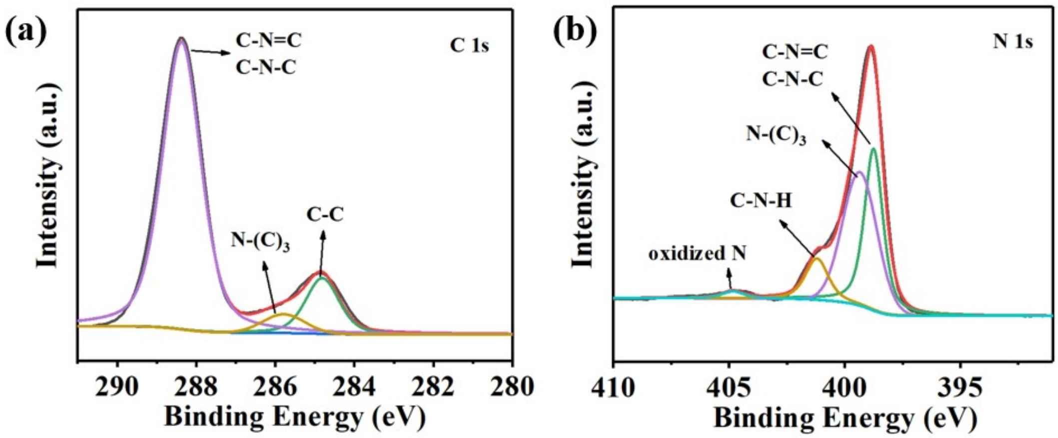


Figure S7. a) C 1s, b) N 1s XPS spectra of bare g-$C_3N_4$.

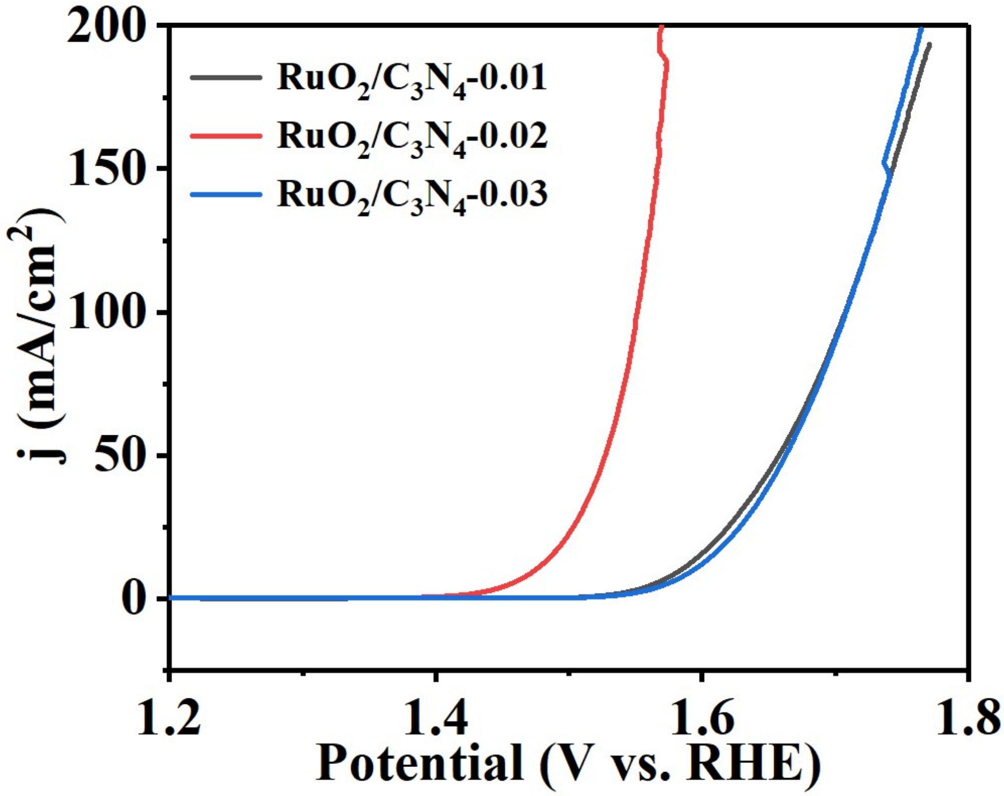

Figure S8. Polarization curves of catalysts with different ratios for OER.

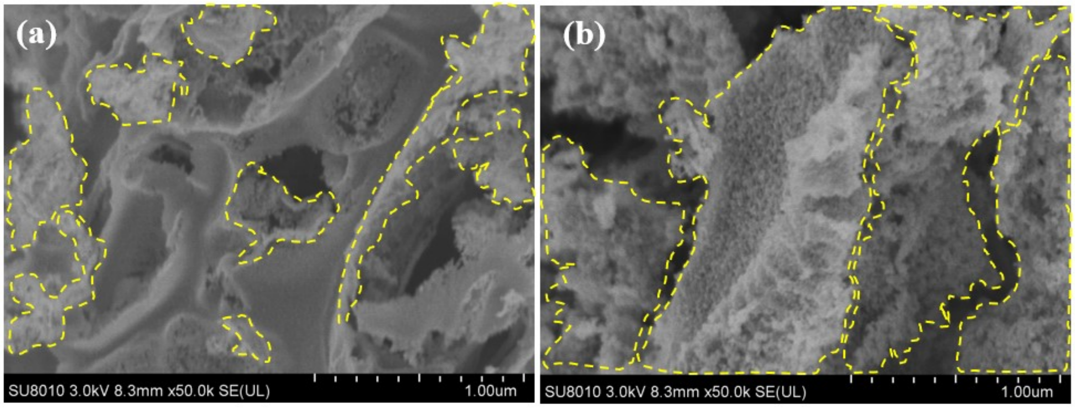

Figure S9. a) SEM image of $RuO_2/C_3N_4$-0.01, b) SEM image of $RuO_2/C_3N_4$-0.03.

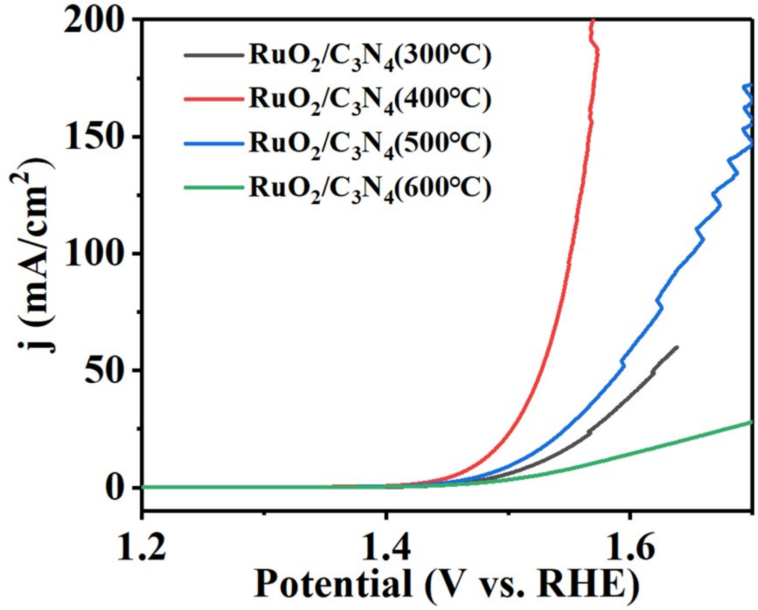


Figure S10. Polarization curves of OER for catalysts with different annealing temperatures.

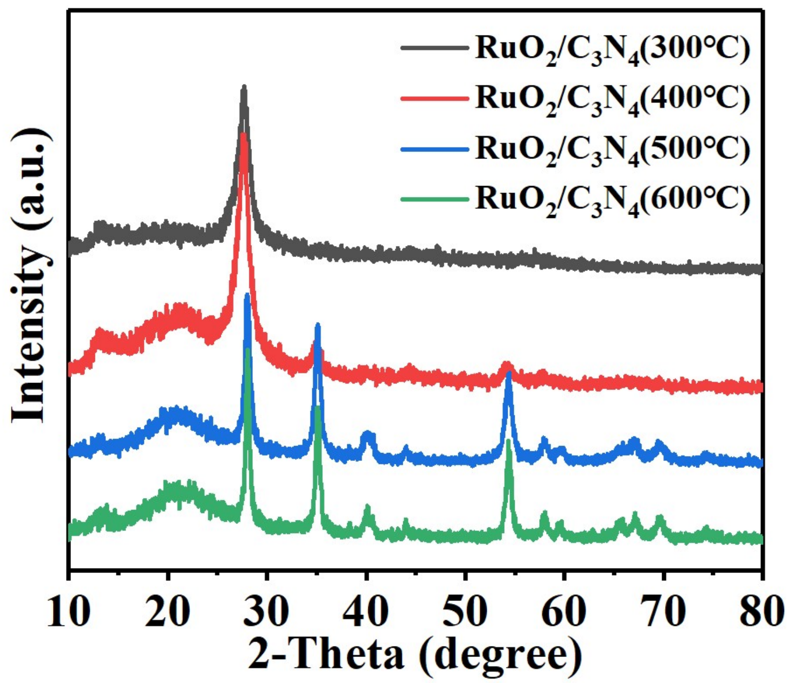


Figure S11. XRD image of $RuO_2/C_3N_4$ at different calcination temperatures.

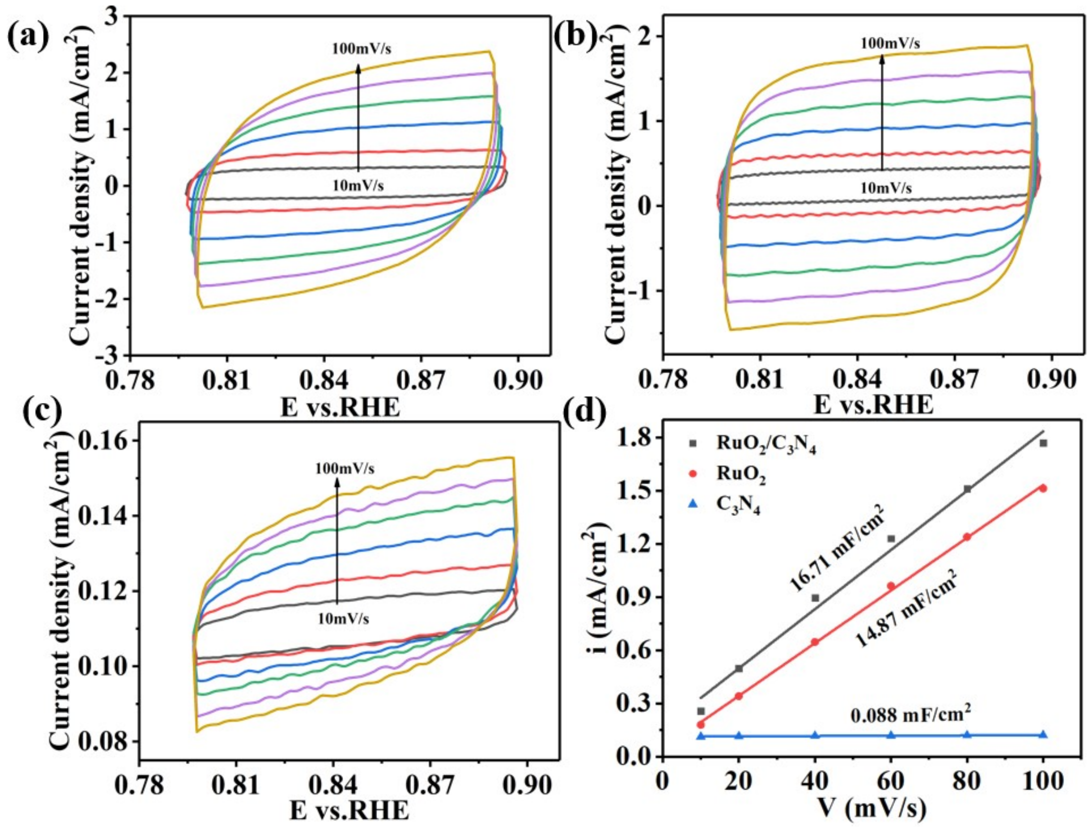


Figure S12. CV curves of a) $RuO_2/C_3N_4$, b) $RuO_2$, c) $C_3N_4$, d) Current density as a function of the scan rate for $RuO_2/C_3N_4$, $RuO_2$ and g-$C_3N_4$ for OER.

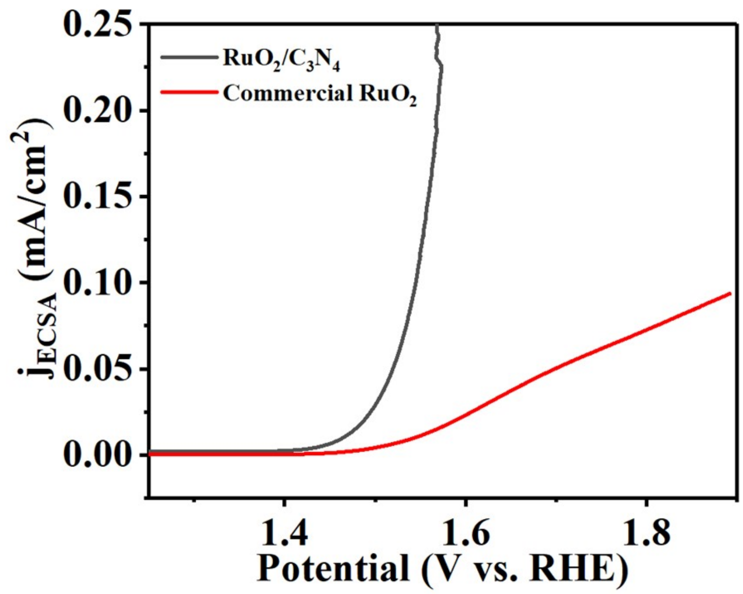

Figure S13. ECSA based LSV of $RuO_2/C_3N_4$ and commercial $RuO_2$ for OER.

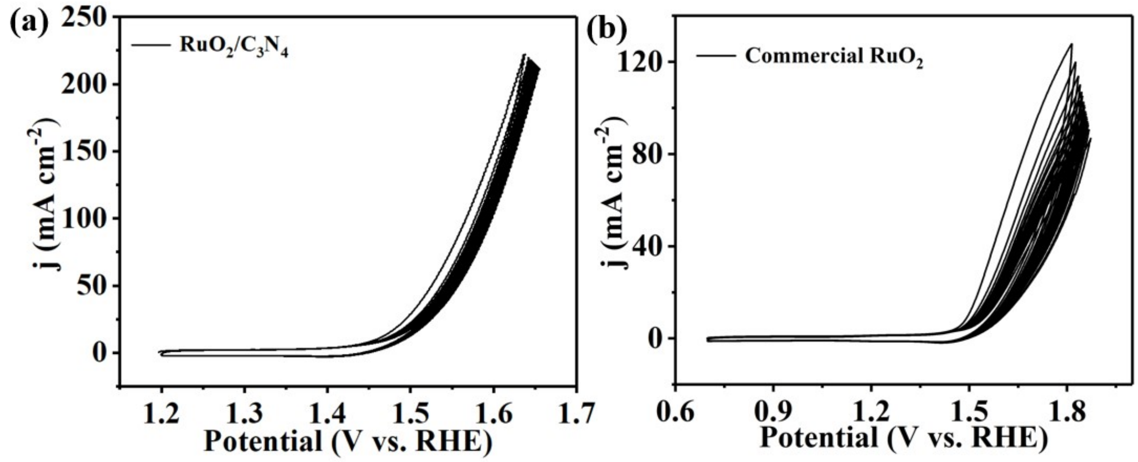


Figure S14. CV curves of a) $RuO_2/C_3N_4$, b) commercial $RuO_2$.

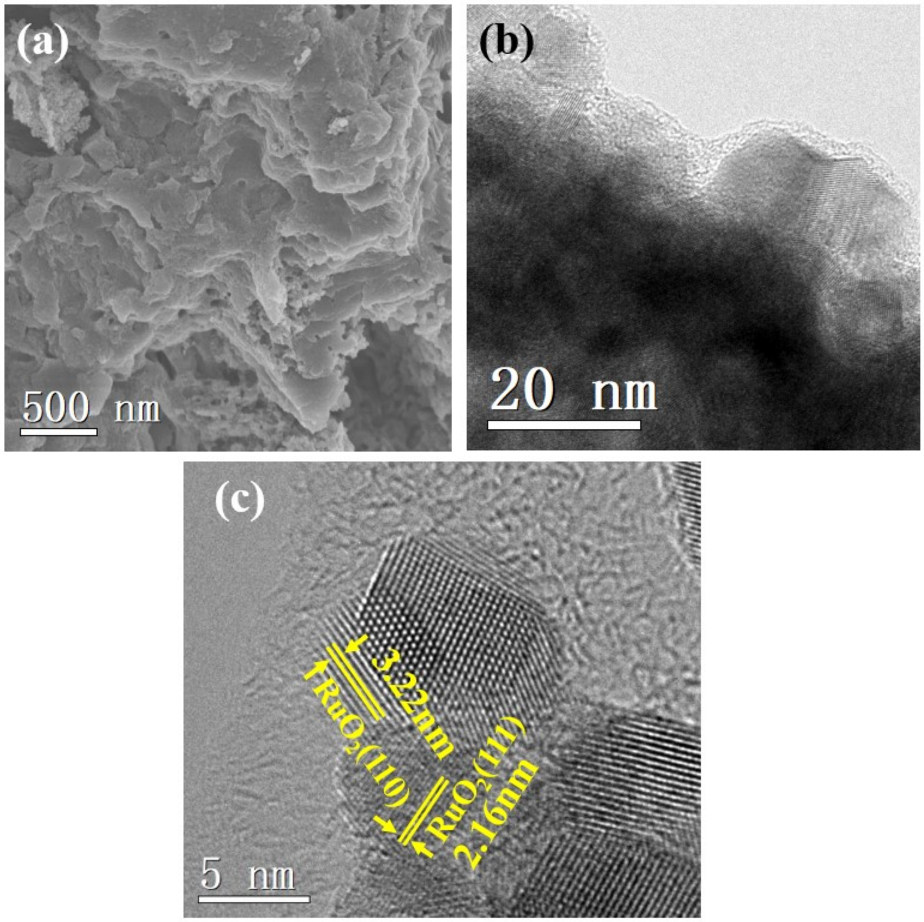


Figure S15. a) SEM image, b) TEM image, c) HRTEM image of $RuO_2/C_3N_4$ after long time chronopotentiometry test.

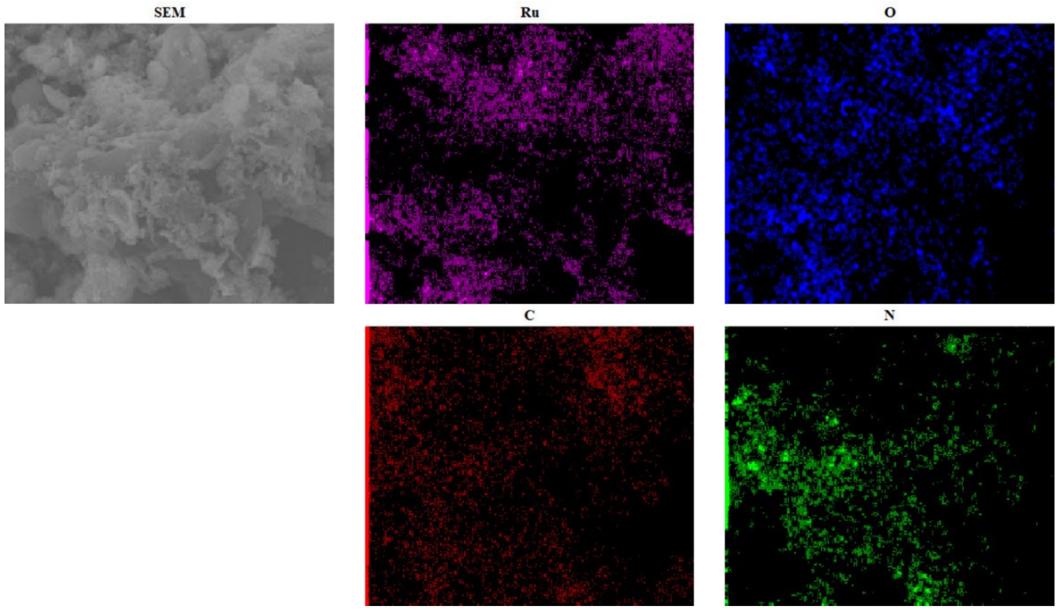

Figure S16. SEM-EDS element mappings of $RuO_2/C_3N_4$ after long time chronopotentiometry test.

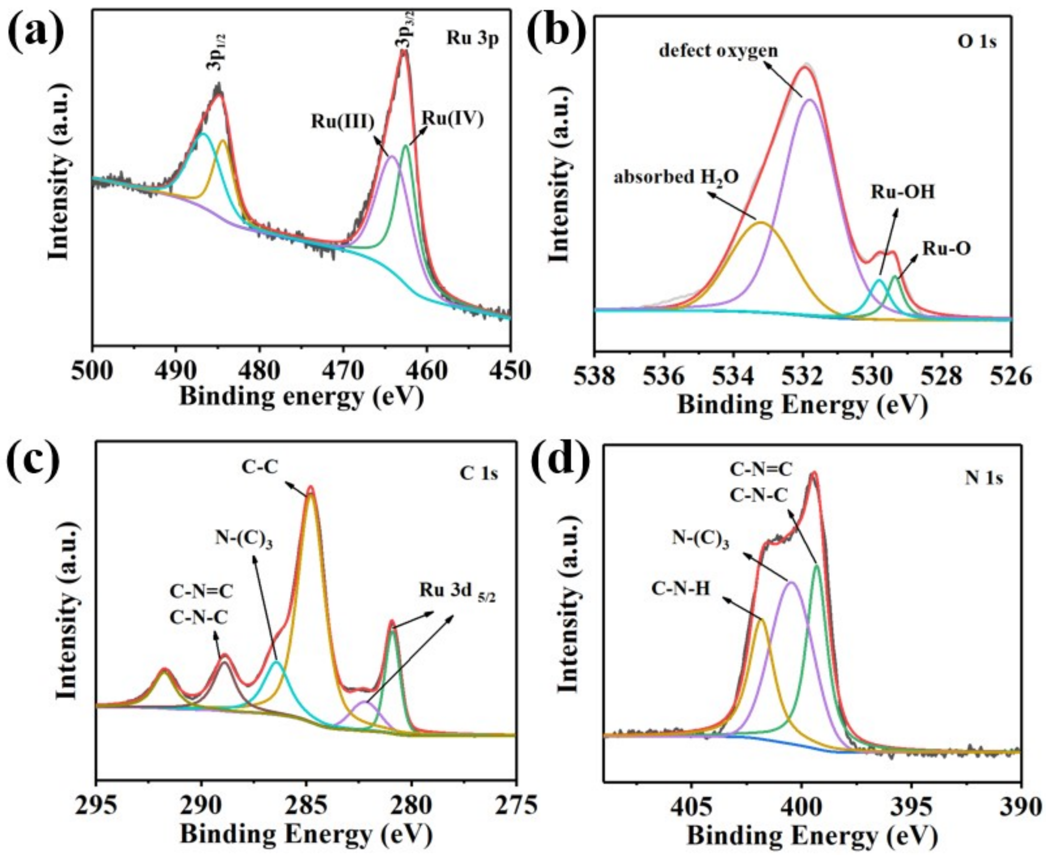


Figure S17. a) Ru 3p, b) O 1s, c) C 1s and d) N 1s XPS spectra of $RuO_2/C_3N_4$ after long time chronopotentiometry test.

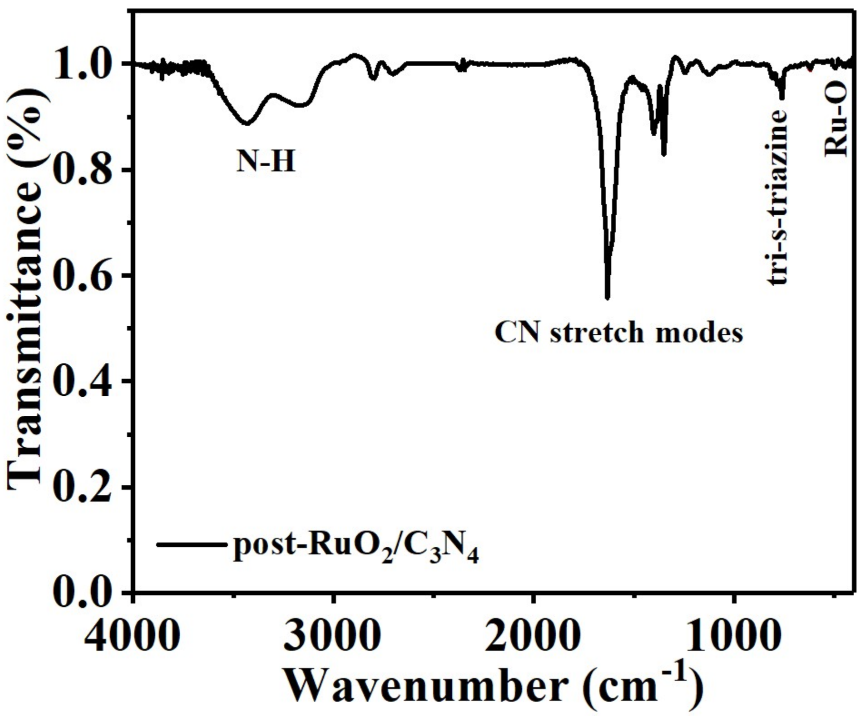

Figure S18. FT-IR spectra of $RuO_2/C_3N_4$ after chronopotentiometry test.

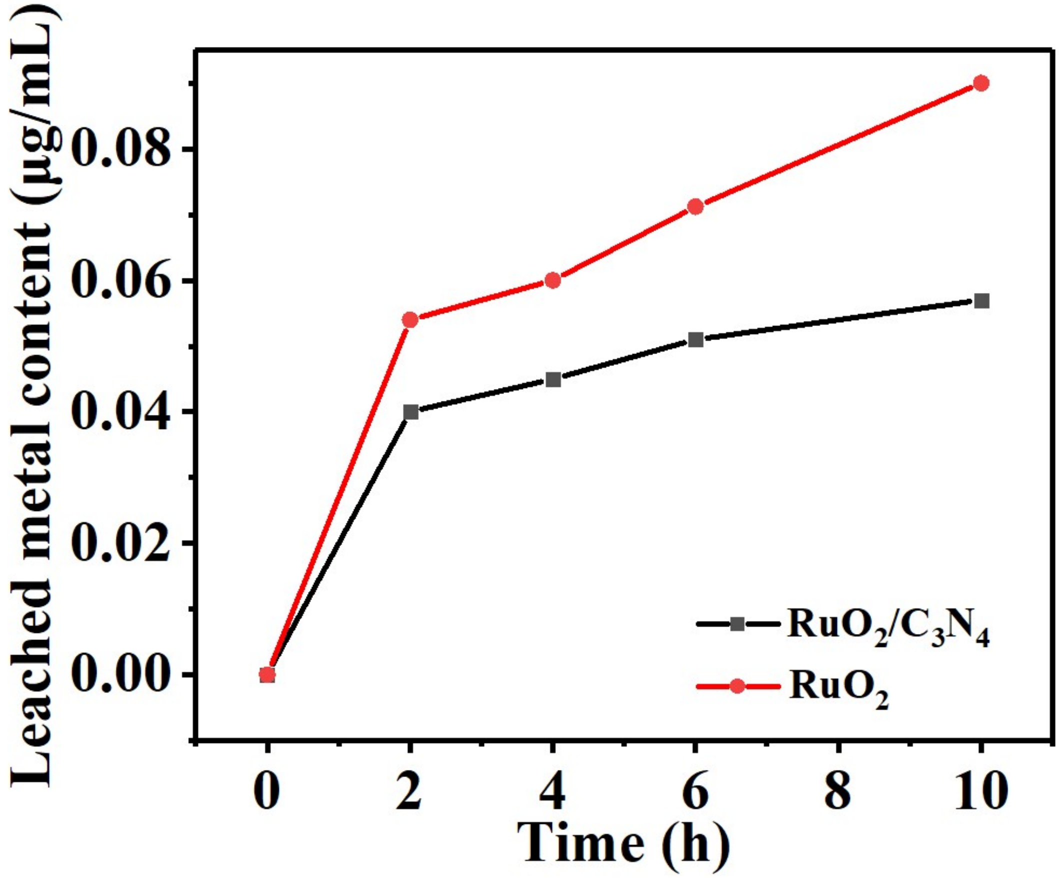

Figure S19. The Ru content in electrolyte after chronopotentiometry test at 10 $mA/cm^2$.

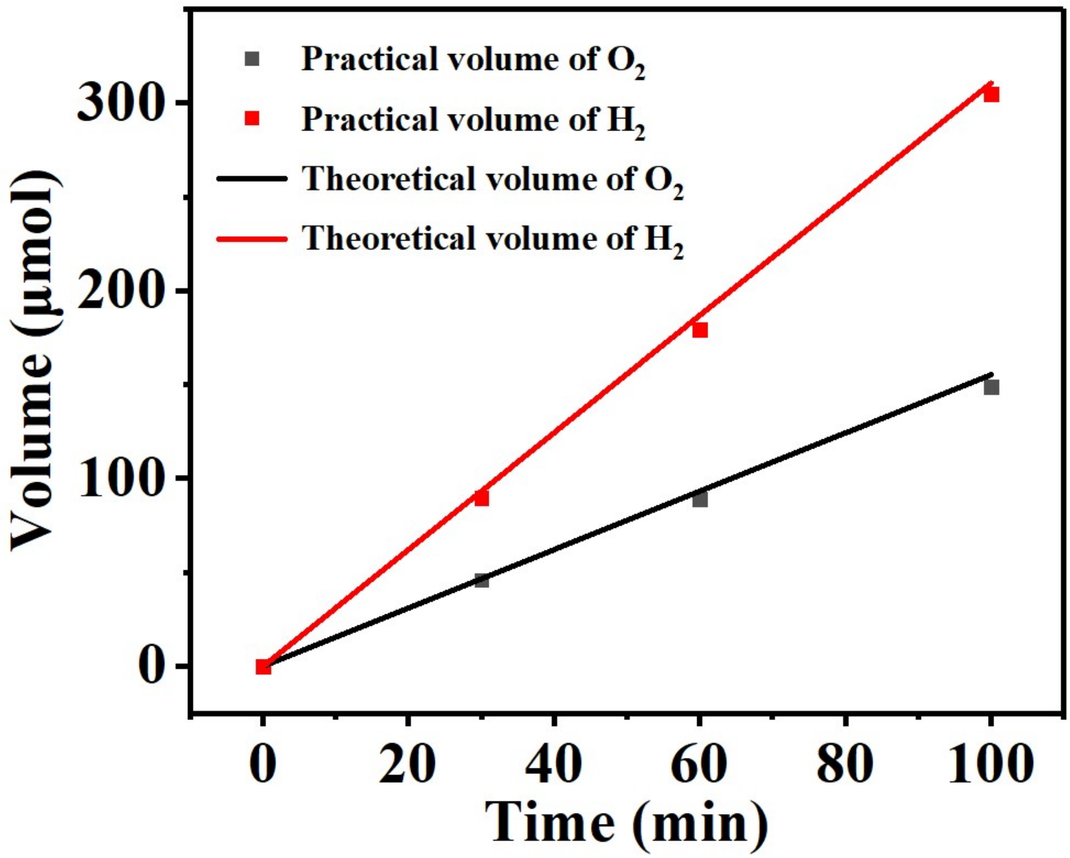


Figure S20. The volume of $O_2$ and $H_2$ produced by $RuO_2/C_3N_4$ in 0.5 M $H_2SO_4$.

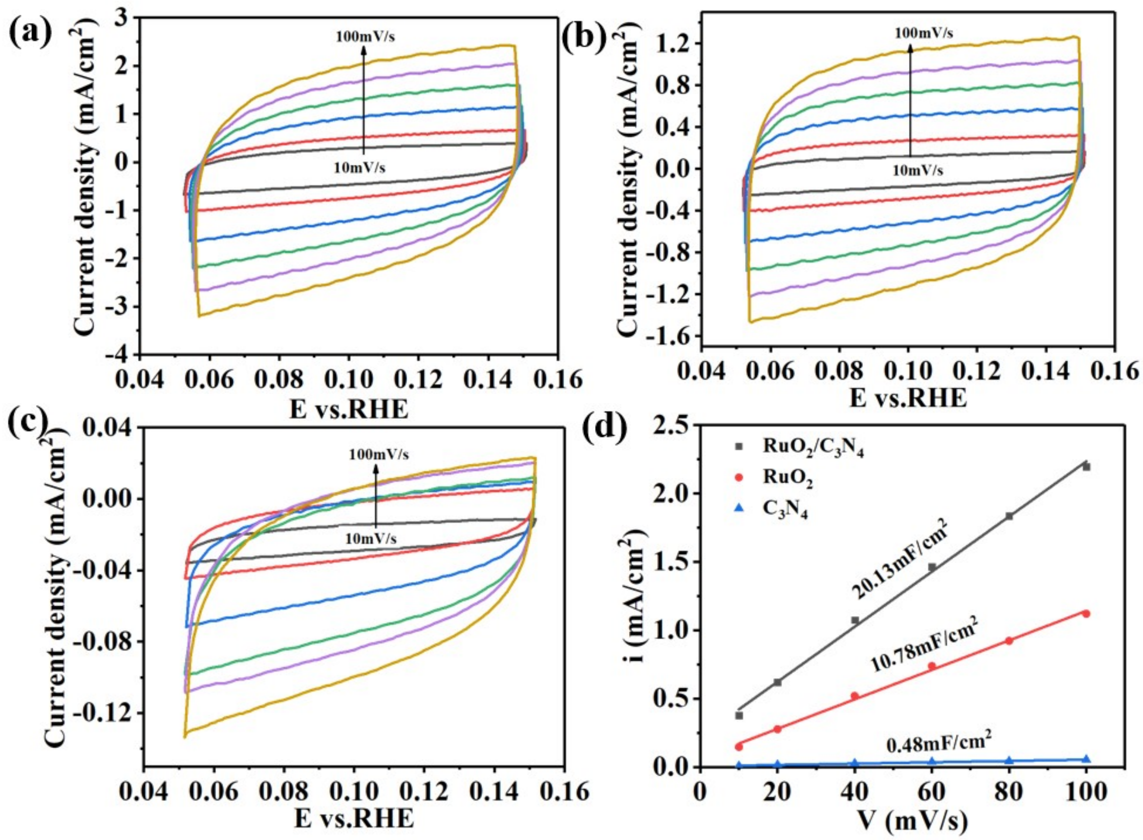


Figure S21. CV curves of a) $RuO_2/C_3N_4$, b) $RuO_2$, c) $C_3N_4$, d) Current density as a function of the scan rate for $RuO_2/C_3N_4$, $RuO_2$ and $C_3N_4$ for HER.

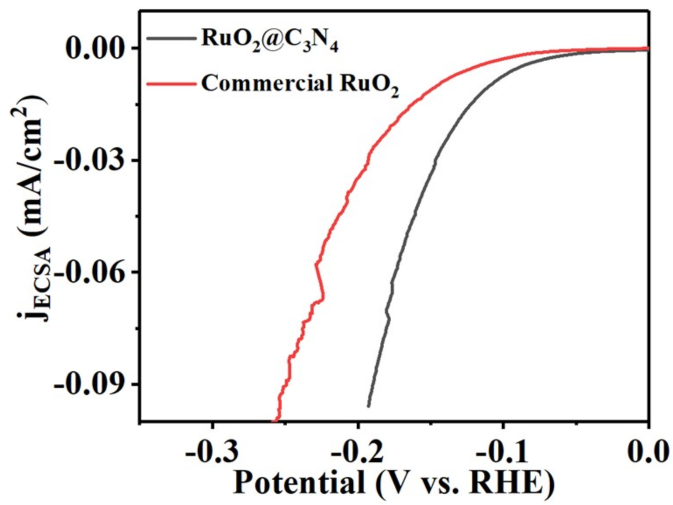

Figure S22. ECSA based LSV of $RuO_2/C_3N_4$ and commercial $RuO_2$ for HER.

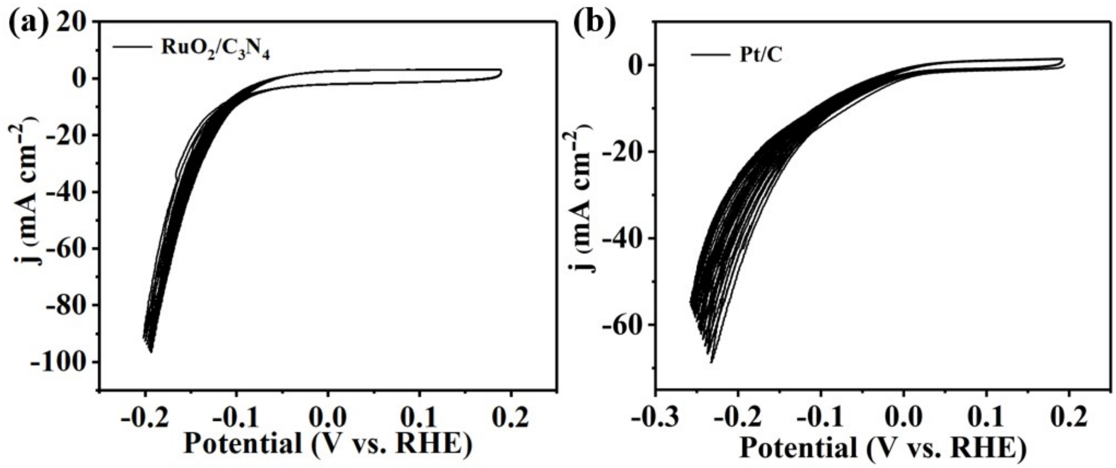


Figure S23. CV curves of a) $RuO_2/C_3N_4$, b) Pt/C.

Table S1. The ECSA of $RuO_2/C_3N_4$, $RuO_2$ and g-$C_3N_4$ for OER

| **catalyst** | **ECSA/$cm^2mg^{-1}$** | **$C_{dl}$/$mFcm^{-2}$** |
|---|---|---|
| $RuO_2/C_3N_4$ | 835.5 | 16.71 |
| $RuO_2$ | 743.5 | 14.87 |
| g-$C_3N_4$ | 4.4 | 0.088 |

Table S2. Summary of recently reported OER electrocatalysts

| **Catalysts** | **Electrolyte** | **η (mV) @10mAcm$^{-2}$** | **Reference** |
|---|---|---|---|
| **$RuO_2/C_3N_4$** | **0.5 M $H_2SO_4$** | **240** | **This work** |
| Ni-$RuO_2$ | 0.5 M $H_2SO_4$ | 214 | *Nat. Mater.*[1] |
| $RuO_2$@/$(Co,Mn)_3O_4$ | 0.5 M $H_2SO_4$ | 270 | *Appl. Catal. B. Environ.*[2] |
| UfD-$RuO_2$ | 0.5 M $H_2SO_4$ | 179 | *Adv. Energy Mater.*[3] |
| BCC-Cr-$SrIrO_3$ | 0.1 M $HClO_4$ | 217 | *Nano Energy*.[4] |
| RuCu NSs/C | 0.5 M $H_2SO_4$ | 236 | *Angew. Chem. Int. Ed.*[5] |
| $IrO_x/SrIrO_3$ | 0.5 M $H_2SO_4$ | 270 | *Nat. Commun.*[6] |

Table S3. The ECSA of $RuO_2/C_3N_4$, $RuO_2$ and g-$C_3N_4$ for HER

| **catalyst** | **ECSA/$cm^2mg^{-1}$** | **$C_{dl}$/$mFcm^{-2}$** |
|---|---|---|
| $RuO_2/C_3N_4$ | 1006.5 | 20.13 |
| $RuO_2$ | 539 | 10.78 |
| g-$C_3N_4$ | 48 | 0.48 |

Table S4. Summary of recently reported HER electrocatalysts

| **Catalysts** | **Electrolyte** | **η(mV) @10mAcm$^{-2}$** | **Reference** |
|---|---|---|---|
| **$RuO_2/C_3N_4$** | **0.5 M $H_2SO_4$** | **109** | **This work** |
| 0.4-Ru@NG-750 | 0.5 M $H_2SO_4$ | 90 | *ACS Catal.*[7] |
| $Ru_2P$ | 0.5 M $H_2SO_4$ | 17 | *ACS Nano*[8] |
| rGO-$MoS_2$/Acc-$TiO_2$/C | 0.5 M $H_2SO_4$ | 207 | *J. Mater. Chem. A.*[9] |
| MoP/$Mo_2N$ | 0.5 M $H_2SO_4$ | 89 | *Angew. Chem. Int. Ed.*[10] |
| Ru@WNO-C | 0.5 M $H_2SO_4$ | 172 | *Nano. Energy.*[11] |

| Catalyst | Electrolyte | η /10 mA $cm^{-2}$ | | Cell voltage/V | Reference |
|---|---|---|---|---|---|
| | | OER | HER | | |
| **$RuO_2/C_3N_4$** | **0.5 M $H_2SO_4$** | **240** | **109** | **1.60** | **This work** |
| Ir-SA@Fe@NCNT | 0.5 M $H_2SO_4$ | 250 | 26 | 1.51 | *Nano Lett.*[12] |
| RuIr-NC | 0.05 M $H_2SO_4$ | 165 | 46 | 1.48 | *Nat. Commun.*[13] |
| Ir/GF | 0.5 M $H_2SO_4$ | 290 | 7 | 1.55 | *Nano Energy.*[14] |
| IrCo | 0.1 M $HClO_4$ | 281 | 17 | 1.59 | *ACS Appl. Mater. Interfaces.*[15] |
| NiSe/NF | 1.0 M KOH | 270 | 96 | 1.63 | *Angew. Chem. Int. Ed.*[16] |

Table S5. Summary of recently reported bifunctional electrocatalysts

# References


1. Z. Y. Wu, F. Y. Chen, B. Li, S. W. Yu, Y. Z. Finfrock, D. M. Meira, Q. Q. Yan, P. Zhu, M. X. Chen, T. W. Song, Z. Yin, H. W. Liang, S. Zhang, G. Wang and H. Wang, *Nat. Mater.*, 2023, **22**, 100-108.
2. S. Niu, X.-P. Kong, S. Li, Y. Zhang, J. Wu, W. Zhao and P. Xu, *Appl. Catal. B: Environ.*, 2021, **297**, 120442.
3. R. X. Ge, L. Li, J. W. Su, Y. C. Lin, Z. Q. Tian and L. Chen, *Adv. Energy Mater.*, 2019, **9**, 1901313.
4. X. X. Zhang, H. Su, X. Sun, C. Y. Yang, Y. L. Li, H. Zhang, W. L. Zhou, M. H. Liu, W. R. Cheng, C. Wang, H. J. Wang and Q. H. Liu, *Nano Energy*, 2022, **102**, 107680.
5. Q. Yao, B. Huang, N. Zhang, M. Sun, Q. Shao and X. Huang, *Angew. Chem. Int. Ed.*, 2019, **58**, 13983-13988.
6. L. C. Seitz, C. F. Dickens, K. Nishio, Y. Hikita, J. Montoya, A. Doyle, C. Kirk, A. Vojvodic, H. Y. Hwang, J. K. Norskov and T. F. Jaramillo, *Science*, 2016, **353**, 1011-1014.
7. L. Bai, Z. Y. Duan, X. D. Wen, R. Si, Q. Q. Zhang and J. Q. Guan, *ACS Catal.*, 2019, **9**, 9897-9904.
8. X. Jin, H. Jang, N. Jarulertwathana, M. G. Kim and S. J. Hwang, *ACS Nano*, 2022, **16**, 16452-16461.
9. J. Li, Z. Wen, Z. X. Hui, Z. W. Chen, C. C. Yang and Q. Jiang, *J. Mater. Chem. A*, 2020, **8**, 14223-14233.
10. Y. Gu, A. Wu, Y. Jiao, H. Zheng, X. Wang, Y. Xie, L. Wang, C. Tian and H. Fu, *Angew. Chem. Int. Ed.*, 2021, **60**, 6673-6681.
11. G. Meng, H. Tian, L. Peng, Z. Ma, Y. Chen, C. Chen, Z. Chang, X. Cui and J. Shi, *Nano Energy*, 2021, **80**, 105531.
12. F. Luo, H. Hu, X. Zhao, Z. Yang, Q. Zhang, J. Xu, T. Kaneko, Y. Yoshida, C. Zhu and W. Cai, *Nano Lett.*, 2020, **20**, 2120-2128.
13. D. Wu, K. Kusada, S. Yoshioka, T. Yamamoto, T. Toriyama, S. Matsumura, Y. Chen, O. Seo, J. Kim, C. Song, S. Hiroi, O. Sakata, T. Ina, S. Kawaguchi, Y. Kubota, H. Kobayashi and H. Kitagawa, *Nat. Commun.*, 2021, **12**, 1145.
14. J. Zhang, G. Wang, Z. Q. Liao, P. P. Zhang, F. X. Wang, X. D. Zhuang, E. Zschech and X. L. Feng, *Nano Energy*, 2017, **40**, 27-33.
15. L. Fu, X. Zeng, G. Cheng and W. Luo, *ACS Appl. Mater. Interfaces*, 2018, **10**, 24993-24998.
16. C. Tang, N. Cheng, Z. Pu, W. Xing and X. Sun, *Angew. Chem. Int. Ed.*, 2015, **54**, 9351-9355.